



Research on the variable volume and temperature air supply strategy based on thermal comfort in a vehicle cabin

Zhaoju Qin¹ · Minghui Jia¹ · Junfa Duan¹ · Lijun Wang¹

Received: 24 November 2021 / Accepted: 25 July 2022 / Published online: 26 August 2022
© Akadémiai Kiadó, Budapest, Hungary 2022

Abstract

The traditional thermal environment management of the passenger compartment adopts the unified regulation method. Air distribution formed in this manner often causes thermal comfort and energy consumption problems. In view of the problems of conventional airflow organization, a new air supply strategy-variable air volume and temperature strategy is proposed. In this air supply strategy, variable air volume and variable temperature air supply is carried out according to the characteristics of thermal comfort requirements of passengers in different periods and positions in the cabin. STAR-CCM+ software coupled with THESUES-FE software was implemented and compared with different air supply methods. The performance of the air supply strategy was evaluated based on PMV-PPD evaluation index. The results show that the variable air volume variable temperature air supply strategy has certain advantages and improves the thermal comfort level of the crew cabin. The cooling capacity of the automobile air conditioning is allocated effectively, thus improving the satisfaction of the occupants to the thermal environment. This strategy not only saves energy, but also improves the cooling effect in the cabin.

Keywords Crew cabin · Thermal comfort · Variable air volume variable temperature · PMV-PPD

Introduction

Due to the frequent occurrence of extreme summer heat, the comfort of the thermal environment in the passenger compartment has become a focus of attention for researchers and passengers [1, 2]. Poor airflow organization in the cabin leads to uneven temperature distribution in the cabin, which in turn decreases the thermal comfort level of the occupant cabin [3–5]. The air delivery strategy of automotive air conditioning affects the airflow organization of the passenger compartment [6]. The traditional way of managing the thermal environment of the passenger compartment is to perform uniform regulation, in which the air vents of the passenger compartment adopt a constant velocity and constant temperature air delivery strategy, which not only causes a waste of energy in the vehicle, but also has an impact on the formation of an uncomfortable thermal environment easily [7, 8]. The uncomfortable thermal environment of

the passenger compartment cannot meet the requirements of human thermal comfort and energy-saving operation. Therefore, it is important to study the air supply strategy of the passenger compartment.

The study of air delivery strategies for automotive air conditioning is an important step in improving the level of thermal comfort in the passenger compartment. Sheng Zhang et al. conducted a study on the zoned air supply strategy in the passenger compartment based on the characteristics that the thermal comfort needs of the compartment passengers are different, and the results showed that the zoned air supply strategy for the passenger compartment improved the thermal comfort level of the passenger compartment [9]. Changping Liu [10] et al. concluded that good airflow organization is essential to obtain a thermally comfortable environment, and therefore conducted a study of air supply strategies on human thermal comfort by conducting a comparison of three different air supply strategies (mixed air supply, stratified air supply, and air curtain air supply). Zhiyuan Chang [11] et al. conducted a research work on a new hybrid air supply strategy for subway vehicle air conditioning, the traditional air supply strategy for subway vehicles is to supply air at constant speed and constant temperature through the upper air inlet of the passenger compartment, the airflow

✉ Zhaoju Qin
qinzhaaju2@126.com

¹ School of Mechanical Engineering, North China University of Water Resources and Electric Power, Zhengzhou 450045, China

organization formed in this mode tends to cause thermal comfort and energy consumption problems. Zhiyuan Chang et al. proposed a new hybrid ventilation strategy, which arranges air vents on the upper and bottom of the passenger compartment to achieve hybrid air supply. Compared with the conventional ventilation strategy, the hybrid ventilation has more uniform temperature distribution, better thermal comfort, higher energy utilization efficiency, and lower air supply short circuit, which improves the thermal comfort level in the cabin. Yongzhi Zhang [12] et al. in a study comparing the effects of hybrid and displacement ventilation strategies on thermal comfort based on the characteristics of airflow organization in a passenger compartment model. The results showed that displacement ventilation has high ventilation efficiency and high energy efficiency, and that hybrid ventilation causes heat accumulation in the passenger compartment. The study also found that the use of multiple air inlets can improve the uniformity of air temperature and velocity distribution in the compartment.

EE Khalil et al. studied the effect of the thermal environment in the occupant compartment of a private car on occupant thermal sensation during hot weather [13]. LI Scurtu et al. investigated the effect of airflow organization in the passenger compartment on occupant thermal sensation by means of numerical simulations [14]. D Lee et al. investigated the effect of different shapes of air vents on the thermal environment of the occupant compartment by comparing the airflow organization effects of focused and diffused air vents [15]. Y Shin et al. studied the cooling process of the passenger compartment based on the physiological temperature response of the driver [16]. C Song et al. investigated the effect of air exit velocity on passenger thermal sensation in a non-homogeneous thermal environment under the influence of solar radiation [17]. K Ravindra et al. studied the thermal comfort parameters of different vehicle models in hot weather [18]. HE Yan-song et al. studied the distribution of cabin temperature and human surface temperature in a non-homogeneous thermal environment and evaluated the passenger compartment according to the temperature distribution [19]. T Hirn et al. studied the effect of different radiation types on the thermal environment of the passenger compartment [20]. However, most of the air supply strategies used in the above studies are constant velocity and constant temperature air supply strategies, which improve the thermal comfort level of the passenger compartment, but do not take into account the human body's demand for thermal comfort at different times as the thermal environment in the compartment changes, and there is less research on variable air volume and temperature air supply strategies for the passenger compartment.

Many topics have investigated the effects of different factors on the thermal environment of the occupant compartment based on the PMV index, which combines human

factors and environmental factors, which generally include ambient temperature, solar radiation, and compartment wind speed [21–23]. JörgSchminder et al. studied the effect of dry and wet bulb air temperature in the cabin on the PMV index [24]. V Norrefeldt et al. studied the effect of airflow recirculation on thermal comfort in the cabin [25]. Xiaojie Zhou et al. studied the effect of solar radiation on passenger thermal sensation under real operating conditions based on PMV index [26]. PA Danca et al. analyzed and compared the thermal environment of the passenger compartment based on the PMV index, comparing the thermal sensation of the passenger in the vehicle under sunlight and shade [27]. W Qingqing et al. studied the thermal environment of the passenger compartment under driving and no-load conditions and found that PMV can accurately reflect the thermal sensation of the occupants under driving conditions in summer, but there is a certain bias in PMV under winter driving conditions [28]. Human factors generally include clothing garment resistance and human metabolism, etc. [29–33]. S Zhang et al. investigated the effects of factors such as clothing garment resistance and human metabolic level on occupant thermal sensation based on PMV-PPD index [34]. P Danca et al. studied the changes in the thermal environment of the cabin with and without occupants in the passenger compartment based on the PMV index [35].

Management of the thermal environment, the traditional approach taken is unified regulation, although the cooling achieved, but there are still certain problems, including the following aspects [36–40]: (1) uneven cooling and heating; (2) unreasonable operation methods, resulting in the waste of energy; (3) low level of design planning. In response to the problems of the traditional air supply strategy, the air supply control system with variable air volume and temperature uses intermittent control of air supply to reduce the waste of energy.

The PMV-PPD index [21–35] was proposed in the early 1970s and has been continuously supplemented and developed and has been recognized by ISO in terms of thermal comfort evaluation criteria, becoming a thermal comfort evaluation criterion of universal significance. The PMV index is mainly the response of the vast majority of people to a thermal environment under the conditions of the same environment, indicating the vast majority of people's recognition of the comfort level of that environment. According to the literature study, it is known that the PMV index is more accurate in predicting the thermal environment evaluation of air conditioning cooling in closed spaces, and the index has a certain degree of deviation in the evaluation of thermal environment under the condition of natural ventilation. In this paper, an air supply strategy with variable air volume and variable temperature is proposed on the basis of the traditional ventilation method for automotive air conditioning systems. Based on the PMV-PPD thermal comfort

evaluation index, the airflow organization characteristics of this air supply strategy are evaluated and compared with several conventional air outlet strategies.

Research methods

Passenger compartment model

In this paper, a six-seat passenger car is used as the object of study to test the thermal environment of the passenger compartment, and the test vehicle is shown in Fig. 1a (size specification (L×W×H) is 4780 mm×1837 mm×1730 mm). The test was conducted by measuring and recording the thermal environment parameters in the passenger compartment through the test instrument. During the test, the car is stationary, the environment temperature is 40°C, the humidity is 50%, and the air flow rate is less than 0.1 m s⁻¹. Since the human head is sensitive to temperature changes, a test of human head temperature was conducted.

The human head temperature test uses a thermocouple measurement system to test the temperature of the human head, while using a hot-wire anemometer to test the air-flow velocity at different locations in the cabin, etc. The test instrument monitors the temperature and velocity fields of the passenger compartment, and the monitoring points in the

test are arranged as shown in Fig. 1b. The brief information of each measurement instrument is shown in Table 1. During the test, the car was stationary at 0 km/h and the tester was sitting quietly in the cabin. The test points were laid out according to Fig. 1b and the thermal environment parameters and the tester's head temperature in the cabin were measured using the test apparatus. The test instruments given in Table 1 were calibrated before the test to ensure their proper function and measurement accuracy.

Numerical simulation

Passenger compartment geometry model

In that study, an SUV model is used as the original model in this paper. Fluid simulation software (STAR-CCM+) and thermal analysis software (THESUES-FE) were used to simulate the heat transfer between the computational environment and the occupant compartment and between the occupant compartment and the manikin. In STAR-CCM+ version 12.02.010 and THESUES-FE version 7.1.5, the crew compartment model was built as shown in Fig. 2. The air outlet and passenger distribution of the passenger compartment are shown in Fig. 2. STAR-CCM+ software for flow field analysis and THESUES-FE software for thermal analysis were coupled to perform a comprehensive thermal comfort study

Fig. 1 Real vehicle model and monitoring points. **a** Test vehicle, **b** Distribution of monitoring points

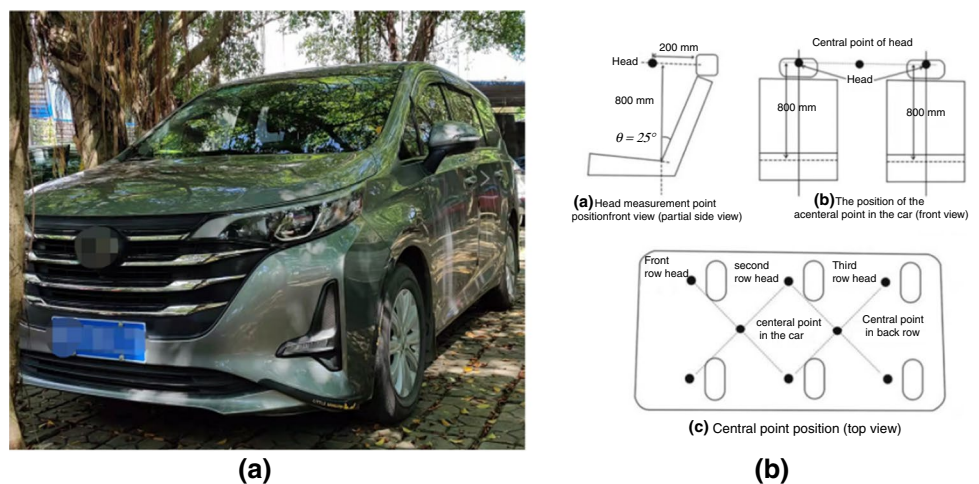
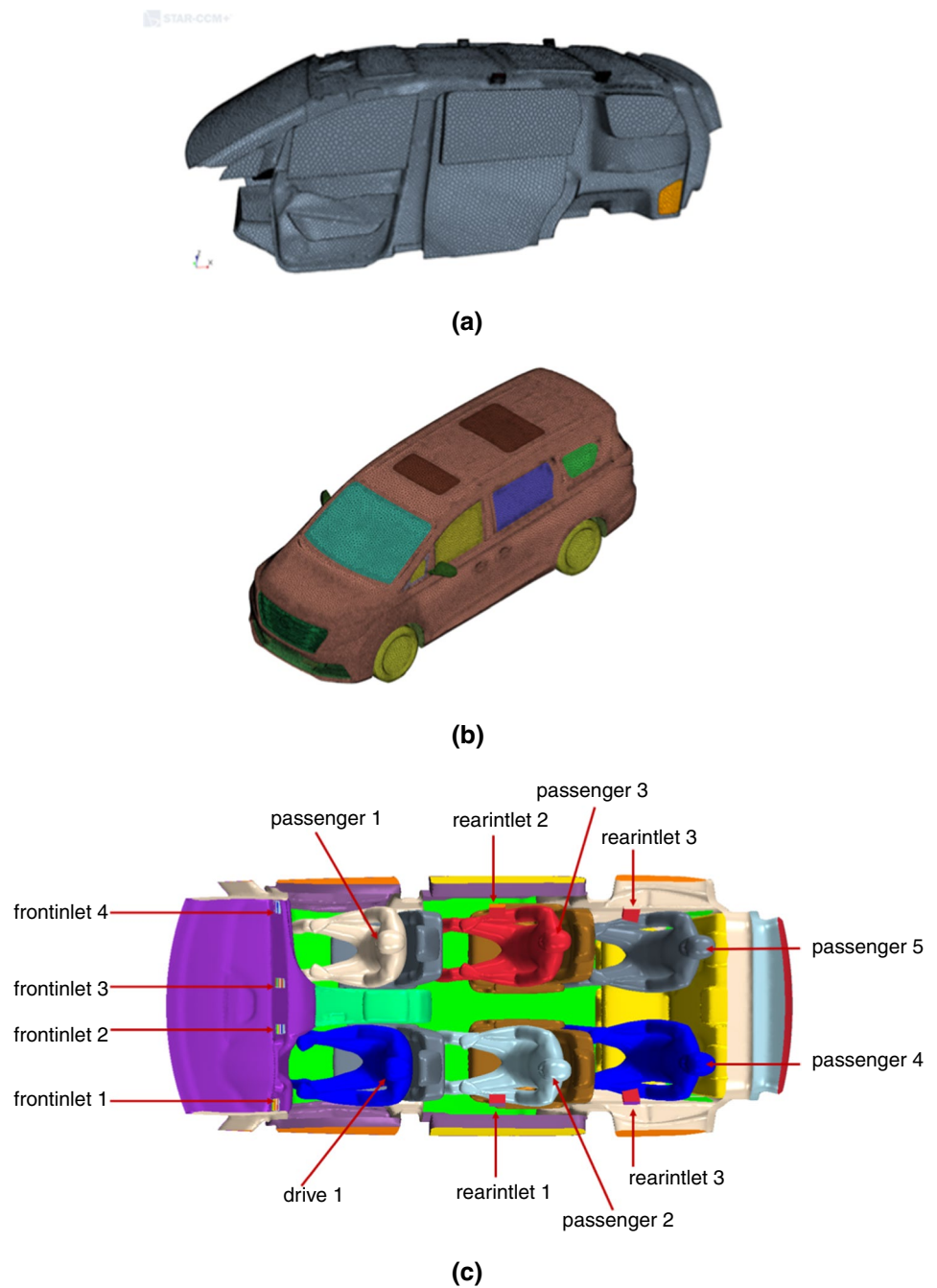


Table 1 Test instrument

Category	Instrument	Machine type	Parameter
Environment temperature/relative humidity	Temperature and humidity measuring instrument	CEM DT-8896	Precision: ± 0.5°C, ± 2%RH
Compartment temperature/relative humidity	Temperature and humidity measuring instrument	CEM DT-8896	Precision: ± 0.5°C, ± 2%RH
Wind speed	Hot-wire anemometer	SMART SENSOR AR866A	Precision: 0.01 m s ⁻¹
Human head temperature	Thermocouple	OMEGA T	Precision: ± 0.2°C

Fig. 2 Passenger compartment model, **a** STAR-CCM+ crew compartment model, **b** THESUES-FE crew compartment model, **c** Air outlet and passenger position distribution



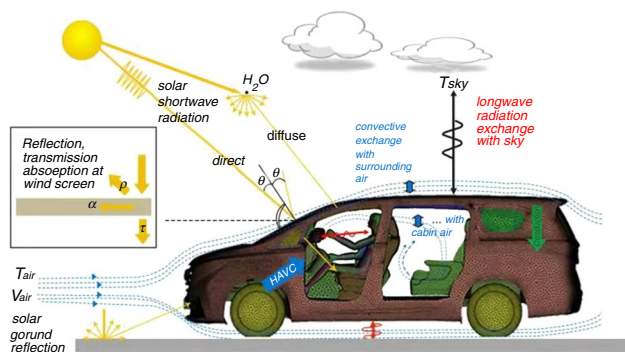


Fig. 3 Heat transfer diagram of passenger compartment

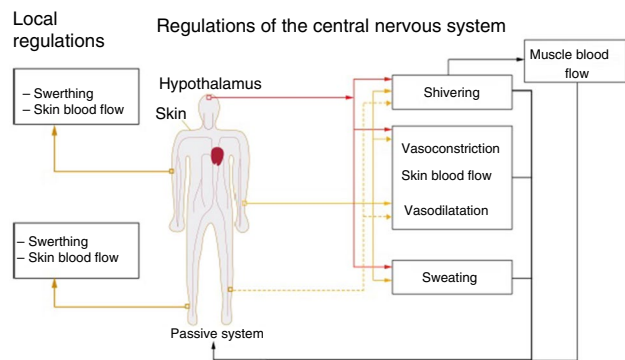


Fig. 4 Model of human body [14]

of the passenger compartment. The model is composed of an occupant compartment and a manikin on each seat (no actual manikin was used in the measurements, just a manikin geometry in the simulations.).

The study included three modes of heat transfer: heat conduction, heat convection, and heat radiation [41]. It includes heat transfer between the mannequin and the thermal environment inside the passenger compartment; convective heat transfer between the low-temperature air supplied from the vehicle air conditioner and the cabin air; heat transfer between the passenger compartment and the environment; and radiation heat transfer from solar radiation to the passenger compartment. Figure 3 shows the heat transfer sketch of the passenger compartment.

Model of human body

In this paper, we chose the FIALA human mathematical model [42], which can be used to predict thermal and

regulatory responses under various environmental conditions. The FIALA human model is a highly complex model that integrates simulated shivering, sweating, and peripheral vasodilatory responses as shown in Fig. 4. The thermal regulation system of the human model carries out the physiological heat load and thermal comfort regulation of the human body under different thermal environments [43, 44].

Human thermoregulation equation

In order to adapt to the surrounding thermal environment, the human body needs to rely on the coordination between the clothing worn on the body and the body's own physiological thermoregulation to achieve the thermal balance that the body needs to maintain to make the body feel thermally comfortable [45]. The body's own thermal regulation is one of the basic functions that the human body has to maintain the body temperature in a relatively stable state to ensure that the body's thermal comfort and other physiological functions are fully functional. The equation of human regulation is as follows [46–48].

$$k \left(\frac{\partial^2 T}{\partial r^2} + \frac{\omega}{r} \frac{\partial T}{\partial r} \right) + \underbrace{q_m}_{\text{metabol}} + \underbrace{\rho_{bl} w_{bl} c_{bl} (T_{bl,a} - T)}_{\text{arterial blood heating}} = \rho c \frac{\partial T}{\partial t} \tag{1}$$

where: ρ is the density of human tissue in kg m^{-3} ; c is the specific heat capacity of human tissue in $\text{J kg}^{-1} \text{ }^\circ\text{C}^{-1}$; T is the temperature of human tissue in $^\circ\text{C}$; k is the thermal conductivity in $\text{W m}^{-1} \text{ }^\circ\text{C}^{-1}$; r is the radial coordinate in m; q_m is the metabolic heat of human body in W. ρ_{bl} is the blood density in kg m^{-3} ; w_{bl} blood perfusion rate in mL min^{-1} ; c_{bl} is the specific heat capacity of blood in kg m^{-3} ; $T_{bl,a}$ is the arterial temperature in $^\circ\text{C}$; t is the time in s.

Solar radiation model

In the car passenger compartment, solar radiation is one of the important influencing factors in the factors affecting the thermal comfort of the car passenger compartment. The hot weather in summer, solar radiation seriously affects its internal thermal environment, leading to a decrease in the level of thermal comfort in the passenger compartment. In THESUES-FE software, make solar radiation settings. Select Solar Loads to set the physical quantities such as direct intensity, azimuth, and altitude angle that characterize the solar radiation intensity for the entire passenger compartment environment. The definition of external solar

radiation intensity is accomplished through the setting of physical quantities related to solar radiation.

Radiation heat transfer takes place in different directions, and for emitting, scattering, and absorbing media, the equation for radiation transfer at position r along direction s is [49, 50].

$$\frac{dI(\vec{r}, \vec{s})}{ds} + (a + \sigma_s)I(\vec{r}, \vec{s}) = an^2 \frac{\sigma T^4}{\pi} + \frac{\sigma_s}{4\pi} \int_0^{4\pi} I(\vec{r}, \vec{s})\phi(\vec{s}, \vec{s}')d\Omega' \tag{2}$$

where: \vec{r} is the position vector; \vec{s} is the direction vector; I is the radiation intensity; depends on the position \vec{r} and direction \vec{s} ; s is the travel length; a is the absorption coefficient; σ_s is the scattering coefficient; n is the refraction coefficient; \vec{s}' is the scattering direction vector; σ is the Stephen Boltzmann constant ($5.672 \times 10^{-8} \text{w m}^{-2} \text{K}^{-4}$); T is the local temperature; ϕ is the phase function; Ω' is the space cubic angle.

Boundary conditions

Human body boundary conditions

The passenger compartment is simulated for summer cooling conditions. In summer, the passenger compartment is mainly affected by solar radiation, high-temperature weather, relative humidity and other factors, which mainly affect the thermal environment of the compartment through heat conduction, heat convection, heat radiation, and other ways [46]. There is a physiological regulation system in the human body model (No respiratory details were involved in the measurement of the manikin, and the effect of respiration was negligible.), the human body temperature changes with the change of the thermal environment in the chamber, and the relevant parameters of the human body model are shown in Table 2.

Boundary conditions of the passenger compartment

The physical parameters of the passenger compartment were set in the THESUES-FE software, and the environmental conditions for this simulation are shown in Table 3. The passenger compartment simulates the actual situation of cooling in summer. The thermal environment of the passenger compartment is affected by the environmental factors such as solar radiation 950 W m^{-2} , ambient temperature $40 \text{ }^\circ\text{C}$, and relative humidity 50%. The air outlet is set to the mass flow boundary and the return air outlet is set to the pressure

Table 3 Boundary conditions

Boundary	Parameter
Solar radiation intensity/ Wm^{-2}	950
Sun azimuth angle/ $^\circ$	0
Sun altitude angle/ $^\circ$	90
Ground reflectance	0.2
Environmental temperature/ $^\circ\text{C}$	40
Environment humidity/%	50
Sky mean radiant temperature/ $^\circ\text{C}$	13.2
Speed of a motor vehicle/ kmh^{-1}	120

outlet boundary [46] (The boundary condition setting of the air inlet and outlet in this paper is based on the relevant references).

Control equation

The simulations were performed using an implicitly indefinite, incompressible, and constant density gas model (The effects of buoyancy were sufficiently small to be ignored [51]). The flow of air and energy transport is controlled by a series of control equations. The Reynolds-averaged Navier–Stokes (RANS) equation and the RNG $k-\epsilon$ turbulence model are suitable for solving air flow and energy transport problems in passenger compartments where the velocity and turbulence of airflow are kept at a relatively low level in the cabin environment [52]. In the case of a constant gas density (i.e., incompressible flow), the rate of change of mass in the control volume with time t is balanced by the net mass flow. The basic control equation is as follows [53]:

Continuity equation:

$$\frac{\partial \rho}{\partial t} + \frac{\partial u}{\partial x} + \frac{\partial v}{\partial y} + \frac{\partial w}{\partial z} = 0 \tag{3}$$

Momentum equation:

$$\begin{cases} \frac{\partial(\rho u)}{\partial t} + \nabla \cdot (\rho u \vec{V}) = -\frac{\partial p}{\partial x} + \nabla \cdot (\mu \text{grad}u) + S_x \\ \frac{\partial(\rho v)}{\partial t} + \nabla \cdot (\rho v \vec{V}) = -\frac{\partial p}{\partial y} + \nabla \cdot (\mu \text{grad}v) + S_y \\ \frac{\partial(\rho w)}{\partial t} + \nabla \cdot (\rho w \vec{V}) = -\frac{\partial p}{\partial z} + \nabla \cdot (\mu \text{grad}w) + S_z \end{cases} \tag{4}$$

Energy equation:

Table 2 Human model parameters

Mass/kg	Height/m	Skin area/ m^2	Metabolism/W at neutrality	Body fat/%	Clothing resistance/clo	Activity/act
73.5	1.71	1.77	87.1	14.4	0.6	1

$$\frac{\partial(\rho T)}{\partial t} + \nabla \cdot (\rho T \vec{V}) = \nabla \cdot \left(\frac{\lambda}{c_p} \text{grad}uT \right) + S_T \tag{5}$$

RNG k-ε turbulence equation:

$$\begin{cases} \frac{\partial(\rho k)}{\partial t} + \nabla \cdot (\rho k \vec{V}) = \nabla \cdot [\Gamma_{k2} \text{grad}k] + G_{k2} + G_b - \rho \epsilon - Y_M \\ \frac{\partial(\rho \epsilon)}{\partial t} + \nabla \cdot (\rho \epsilon \vec{V}) = \nabla \cdot [\Gamma_{\epsilon 2} \text{grad}\epsilon] + C_{1\epsilon} \frac{\epsilon}{k} (G_{k2} + C_{3\epsilon} G_b) - C_{2\epsilon} \rho \frac{\epsilon^2}{k} \end{cases} \tag{6}$$

For the RNG k-ε model, the Reynolds averaging method is used, which is able to reflect the changes in the mean flow field caused by the turbulent flow; it also satisfies the required mean physical quantities of the turbulent field and greatly reduces the task and the computational time. The constant terms in the above equations are explicitly listed in some literature.

Airflow organization scheme

For the setting of the inlet temperature, relevant information shows that the air outlet temperature of automobile air conditioner is 5–20°C when the compressor is working, so 5°C, 15°C, and 20°C are chosen as the air supply temperature for the study in the calculation and simulation. In order to compare the difference between this strategy and the conventional strategy (Frontinlet: frontinlet1~frontinlet4, Rearinlet: rearinlet1~rearinlet4.), four simulation schemes were developed as shown in Table 4 (According to the requirements of industrial partners, the air outlet temperature range is 4–20 °C.). In general, each passenger can inhale at least 250 g of fresh air per minute [53], and the boundary conditions of the air outlet in this paper draws on the way the relevant literature is set up, while the air outlet parameters draw on the relevant parameters from the relevant literature [46].).

Table 4 Different air outlet schemes

Scheme	Characteristics	Time/s	Temperature/°C	Mass flow rate/kg·s ⁻¹	
				Frontinlet	Rearinlet
Scheme 1	Variable air volume and temperature	0~1800	6	0.2	0.1
		1800~3600	11	0.16	0.08
		3600~5400	16	0.12	0.06
Scheme 2	Variable temperature	0~1800	6	0.2	0.1
		1800~3600	11		
		3600~5400	16		
Scheme 3	Variable air rate	0~1800	6	0.2	0.1
		1800~3600		0.16	0.08
		3600~5400		0.12	0.06
Scheme 4	Constant speed constant temperature	0~5400	6	0.2	0.1

Table 5 PMV evaluation index

Cold	Cool	Slightly cool	Neutral	Slightly warm	Warm	Hot
-3	-2	-1	0	1	2	3

PMV-PPD evaluation index

PMV evaluation index

PMV evaluation index: predicted mean vote, which is a common standard for thermal comfort evaluation and recognized by the thermal environment evaluation industry, involves a mathematical model of the interaction of six main factors such as ambient temperature, mean radiation temperature, relative humidity, human metabolism, clothing resistance, and cabin wind speed [21]. The PMV index is divided into seven evaluation levels as shown in Table 5 [35].

The mathematical expression of PMV is as follows:

$$PMV = f(I_{cl}, M, t_a, t_r, V_a, P_a) \tag{7}$$

where *M* is the human energy metabolic rate in W m⁻²; *t_a* is the air temperature around the human body in °C; *t_r* is the average indoor radiation temperature in °C; *t_r* is the average radiation temperature in °C; *V_a* is the cabin air velocity in m s⁻¹; *I_{cl}* is the clothing thermal resistance in clo, *P_a* is the partial pressure of water vapor around the human body in Pa.

PPD evaluation index

PPD evaluation index [21]: Predict the percentage of people who are dissatisfied with the thermal environment. In the same space, there are differences in people’s evaluation of the thermal environment, and the PMV evaluation index cannot accurately predict everyone’s thermal sensation of the thermal environment, so the PPD evaluation index is needed to make up for it and improve the accurate prediction

of the thermal environment. The mathematical expression for the mutual coupling of PMV and PPD is as follows:

$$PPD = 100 - 95 \times e^{-(0.03353 \times PMV^4 + 0.2179 \times PMV^2)} \quad (8)$$

According to ISO7730 standard [54], the thermal comfort range is determined as: $-0.5 < PMV < +0.5$, $-10\% < PPD < +10\%$. Within this range, people are satisfied with and agree with the thermal environment. For PMV, PPD indicators (PMV is used in CFD calculations and the Mean radiation temperature can be obtained in CFD calculations) are available in software post-processing after simulation calculation iterations.

Control principle of variable air volume and temperature air supply strategy

With the development of multi-zone variable air volume variable temperature air supply systems, this has brought about an impact on the implementation of traditional

centralized and constant temperature air supply strategies [36]. The schematic diagram of the variable air volume and temperature air supply strategy is shown in Fig. 5. The strategy is based on the differences between air supply time, air supply interval, and air supply temperature, which can not only make full use of the vehicle energy, but also reduce the waste of resources and environmental pollution (The air supply is divided into three different stages according to the air conditioning operation time, supply early stage: 0–1800s, Supply middle stage: 1801–3600 s, Supply late stage: 3601–5400 s; the air supply temperature stage can be divided into three stages according to the air conditioning operation, Cooling early stage: 0–1800s, Cooling middle stage: 1801–3600 s, Cooling last stage: 3601–5400 s).

The control principle of the variable air volume and temperature air supply strategy is shown in Fig. 6. The air supply parameters are set according to the control device at the main links of the system according to the air supply strategy, and the air supply parameters are controlled and corrected by mass flow sensors and temperature sensors.

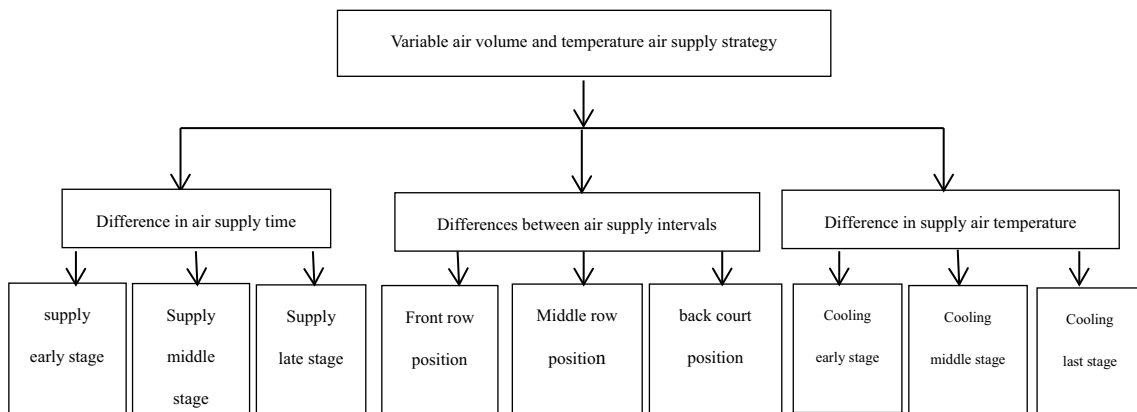


Fig. 5 Diagram of variable air volume and temperature air supply strategy

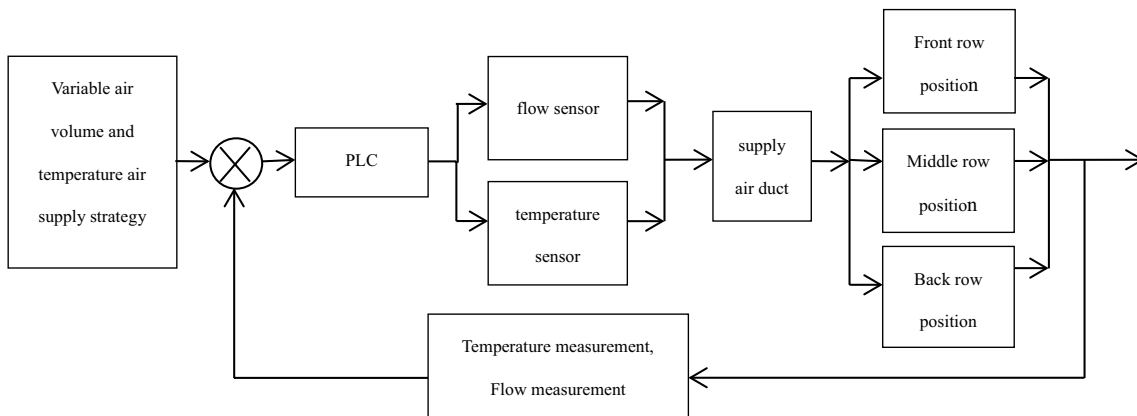


Fig. 6 Control principle of variable air volume and temperature air supply strategy

Air supply ducts are used to supply air to different locations in the passenger compartment. Flow sensors, temperature sensors, wireless data transmission modules, time-of-day controllers, etc. are installed in the air ducts at different locations to process operating parameters and provide feedback on the passenger's status.

Model validation

In order to ensure the validity of the three-dimensional model of the passenger compartment under the current study, thermal comfort tests of the passenger compartment under different operating conditions were carried out, and the calculation model was revised and calibrated according to the test data. The validation conditions were set as shown in Table 6, and the same boundary conditions as the test were chosen for the simulation as shown in Table 7, and the speed of the test vehicle was 120 km/h. When the model was validated, the test conditions were exactly the same as the simulation conditions.

A comparison of the experimental and simulated human head temperature results is shown in Fig. 7. Numerical simulation of the human head temperature and the actual human head temperature error, simulation error within 10%, such an error value can basically meet the accuracy requirements of engineering practice. It can be assumed that the calculation results reflect the changes in the cooling process of the passenger compartment.

Results and discussion

In this section, the simulation results of these four air supply strategies are compared and analyzed, mainly the changes of temperature field, velocity field, and PMV-PPD evaluation index. To facilitate the analysis of the velocity field in the passenger compartment, two special cross sections are intercepted in this paper, and then the velocity field in these sections is analyzed. These two cross sections are normal to [0.0, 1.0, 0.0] and the names of the cross sections are cross Sect. 1 (normal to [2.0, 0.4, 1.0]) and cross Sect. 2, as shown in Fig. 8 (normal to [2.0, -0.4, 1.0]), with each of the two cross sections intersecting the body vertically (in the velocity field results below, cross Sect. 1 is on the left and cross Sect. 2 is on the right.).

Table 7 Boundary conditions for simulation verification

Boundary	Parameter
Solar radiation intensity/W m ⁻²	950
Sun azimuth angle/°	0
Sun altitude angle/°	90
Ground reflectance	0.2
Environmental temperature/°C	40
Environment humidity/%	50
Sky mean radiant temperature/°C	13.2
Speed of a motor vehicle/kmh ⁻¹	120

Velocity field of different air supply strategies

The velocity field distribution of the crew cabin is one of the important indexes affecting the thermal comfort level of the crew cabin. According to the numerical simulation results of simulation calculation, the influence of the velocity field distribution of the crew cabin under different schemes is shown in Fig. 9. In Fig. 9, (a) compares the velocity field of (b). Since (a) adopts the variable air volume variable temperature air supply strategy and (b) adopts the variable temperature constant speed air supply strategy, although (a) initial air supply velocity is 0.2 kg s⁻¹, it can be clearly seen from the velocity field cloud diagram that the peak velocity of (a) is significantly lower than that of (b). And the peak speed of (a) and (b) is 10.73 m s⁻¹, from the air volume can be calculated (a) is less than (b), to a certain extent can save the use of automobile energy. (a) Compared with (c), the same variable air volume strategy was adopted, so the velocity fields of these two schemes were the same. (b) and (d) adopt the constant wind speed supply strategy, and the velocity field of these two air supply schemes is the same.

As a whole, the speed peak with the variable air volume supply strategy is lower than the speed peak with the constant speed supply strategy. The use of variable air volume air supply strategy can save the energy use of the vehicle. The airflow is sent out from the air outlet and blown to the rear of the crew cabin, and the airflow speed inside the entire passenger cabin is distributed in a trend of high and low, and the airflow speed in the rear space is higher than that in the front. The middle and rear row position is close to the air outlet, the peak of the velocity field; the front row position due to the long distance from the air outlet, the airflow has

Table 6 Validation conditions

Categories	Airflow speed	Temperature/°C
Condition 1	frontinlet 1~4: 0.04 kg s ⁻¹ rearinlet 1~4: 0.02 kg s ⁻¹	15
Condition 2	frontinlet 1~4: 0.06 kg s ⁻¹ rearinlet 1~4: 0.03 kg s ⁻¹	15
Condition 3	frontinlet 1~4: 0.08 kg s ⁻¹ rearinlet 1~4: 0.04 kg s ⁻¹	15

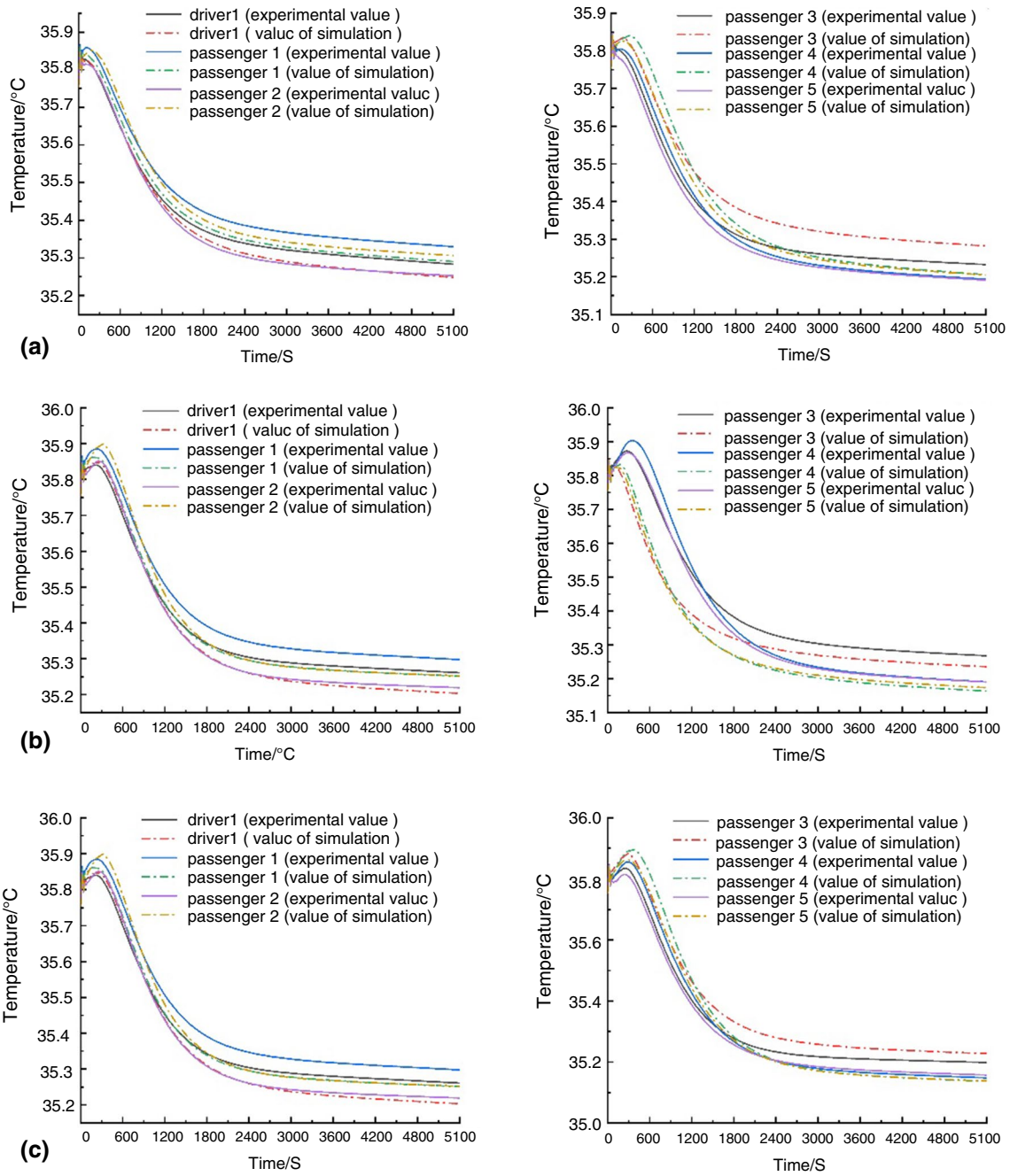


Fig. 7 Comparison of human head temperature test values and simulated values, **a** Condition 1, **b** Condition 2, **c** Condition 3

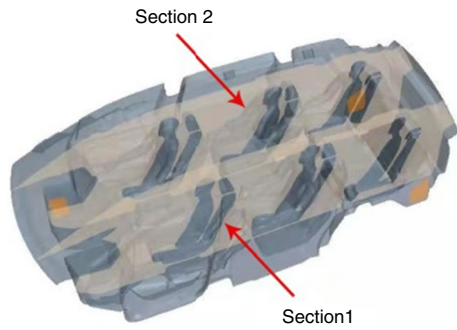


Fig. 8 Sect. 1 and Sect. 2

been dispersed when blowing the human body, did not form a large velocity peak; another reason for the appearance of the passenger compartment velocity field anomaly is due to the spatial distance of the crew cabin limitations, in the cross section is closer to the sidewall air outlet, the air is more concentrated.

Temperature field under different schemes

From Fig. 10, it can be seen that the temperature of the instrument panel in the crew cabin under the four schemes is up to 60 °C or more due to the high temperature of the

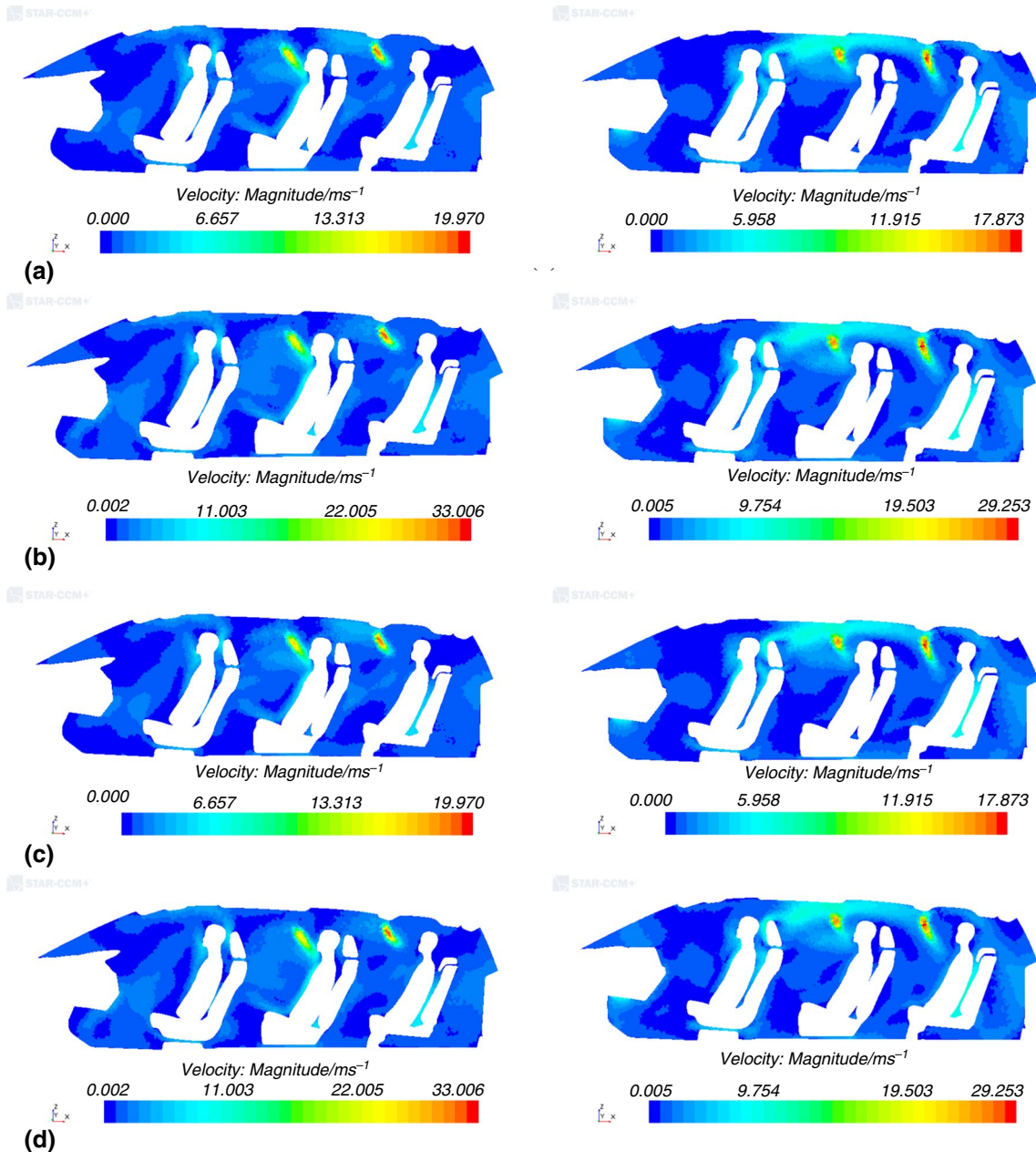


Fig. 9 Velocity fields under different schemes (Solution time: 5400 s), **a** variable air volume and temperature, **b** variable temperature, **c** variable air volume, **d** constant speed and constant temperature

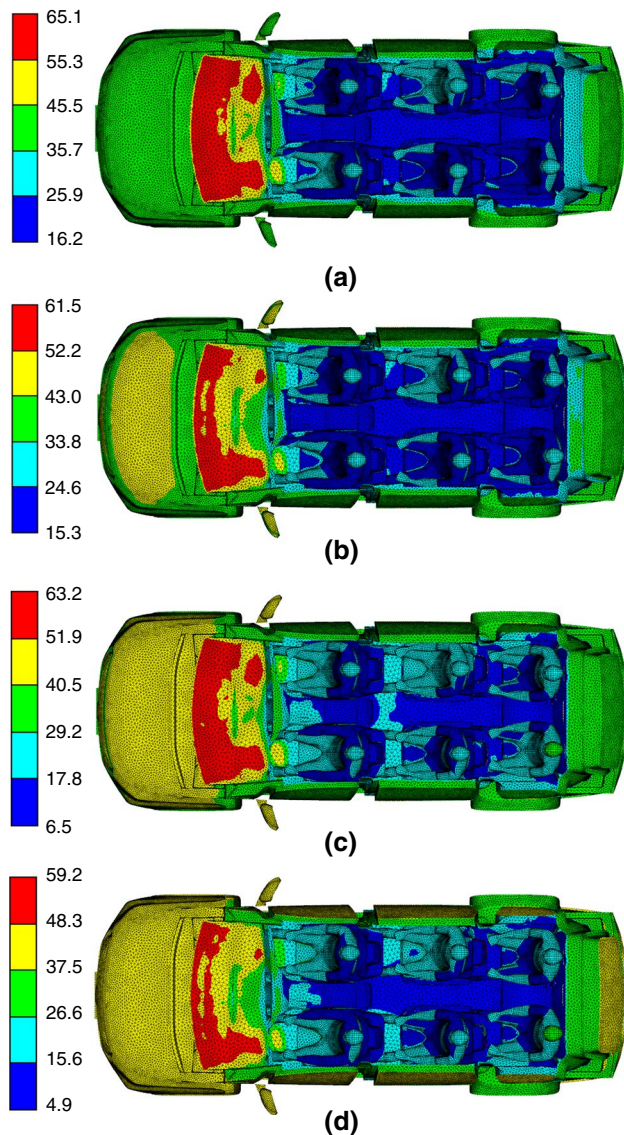


Fig. 10 Temperature field of different schemes (Solution time: 5400 s), **a** variable air volume and temperature, **b** variable temperature, **c** variable air volume, **d** constant speed and constant temperature

engine compartment and solar radiation. By comparing the temperature fields of (a) and (b), the body surface temperature of (a) is higher than the temperature of the active instrument of (b). Due to the variable air volume (VAV) exhaust strategy of (a), passengers are not comfortable due to the air volume. (a) and (c) compare the temperature field, due to the continuous low-temperature air outlet of scheme 3 resulting in a lower temperature in the crew cabin, (a) due to the variable air volume and variable temperature air supply strategy, avoiding the discomfort of the human body in a cold space for a long time. Comparing the temperature fields of (a) and

(d), it is obvious that the temperature of the passenger compartment of scheme 4 is significantly lower than that of (a), and the low-temperature space leads to a reduced experience of people riding in the car.

Comparing the temperature fields of (b) and (d), the cabin temperature of (b) is higher than that of (d). Due to the constant temperature air supply used in (d), the air outlet temperature is 6°C. Due to the prolonged low-temperature air supply, the cabin is over-cooled, resulting in the low temperature of the crew cabin. From Fig. 10, it can be seen that at 5400 s, the mean radiation temperature in the cabin of scheme 1~scheme 4 are 26.5°C, 25.1°C, 20.9°C and 18.5°C, respectively (the average temperature in the cabin can be calculated by CFD).

PMV-PPD evaluation indexes of different schemes

The trend of PMV-PPD indexes of different air supply schemes can be clearly seen from Table 8. The PMV-PPD index of scheme 1 meets the satisfactory thermal comfort range as determined by ISO7730 standard, and the highest level of PMV index of scheme 1 is 0.31 and the lowest level is -0.27, which fully meets the satisfactory thermal comfort range. Comparing scheme 1 and scheme 4, the effect of adopting a variable air volume and temperature air supply strategy on the thermal comfort level of the crew cabin can be clearly seen. Compared to the constant velocity and constant temperature air supply strategy of scheme 4 and, the air supply scheme of scheme 1 not only improves the thermal comfort level of the crew cabin, but also saves the use of energy in the vehicle. The PMV index of scheme 4 is as low as -2.51, and the air supply strategies of schemes 2-3 also improve the thermal comfort level in the cabin compared to scheme 4. The inverse relationship between PMV and PPD can be seen in Fig. 11.

Compared with scheme 2 and scheme 4, the variable temperature air supply strategy can significantly improve the thermal comfort level of the crew cabin. As can be seen from Table 8, in this study, constant temperature and constant speed air delivery caused the cold feeling of the whole passengers, and people were extremely dissatisfied with the thermal environment. The PMV-PPD index of the air supply strategy of scheme 1 is maintained in the range of $-0.5 < \text{PMV} < +0.5$ and $-10\% < \text{PPD} < +10\%$. From the perspective of energy saving and thermal comfort, the constant velocity and constant temperature air supply scheme can no longer meet the needs of thermal comfort of the crew cabin, and the variable air volume and temperature air supply strategy can not only improve the thermal comfort level of the passenger cabin, but also respond to the concept of energy saving and environmental protection.

Table 8 PMV-PPD results under different schemes

Category	Driver1		Passenger1		Passenger2		Passenger3		Passenger4		Passenger5	
	PMV	PPD/%	PMV	PPD/%	PMV	PPD/%	PMV	PPD/%	PMV	PPD/%	PMV	PPD/%
Scheme1	0.31	7.07	0.22	6.01	-0.04	5.03	0.21	6.00	-0.27	6.52	-0.34	7.42
Scheme2	-0.131	5.35	-0.137	5.37	-0.4	8.38	-0.2	5.84	-0.56	11.68	-0.6	12.63
Scheme3	-1.29	39.88	-1.36	43.88	-1.63	58.33	-1.14	32.63	-1.91	72.97	-2.04	78.72
Scheme4	-2.04	78.71	-1.97	75.84	-2.31	88.67	-1.91	72.73	-2.51	93.68	-2.57	94.85

Fig. 11 PMV-PPD results under scheme 1 ~ scheme 4, **a** PMV results, **b** PPD results. (d1: driver1, p1: passenger1, p2:passenger2, p3:passenger3, p4:passenger4, p5:passenger5)

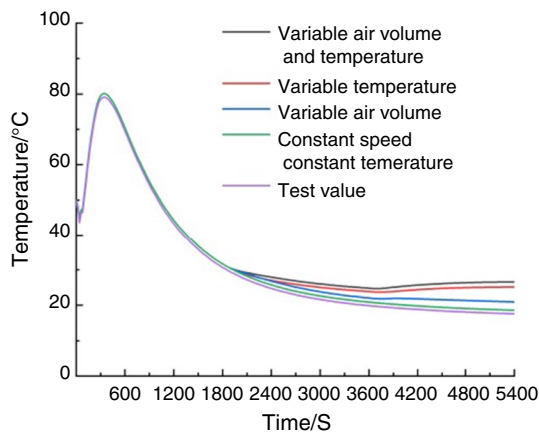
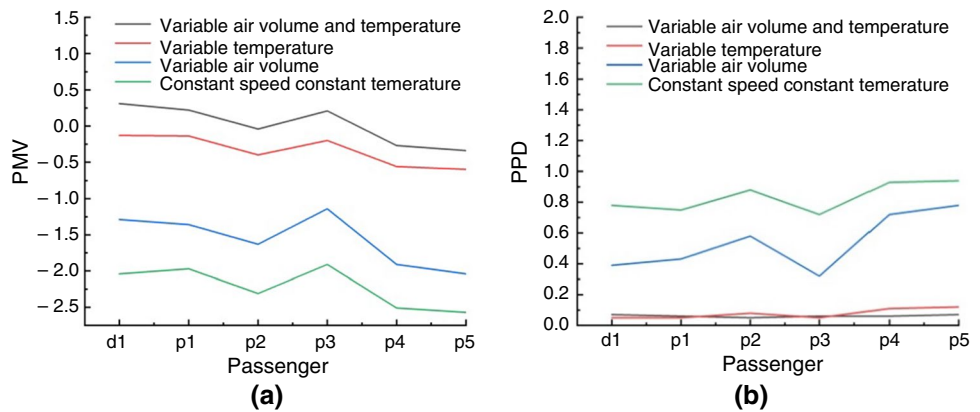


Fig. 12 Average passenger compartment temperature

Variation of human head and cabin temperature under different scheme

From Fig. 12, it can be seen that the average temperature of the passenger compartment has a maximum temperature

fluctuation at about 600 s, which is the result of the uneven mixing of hot and cold air in the crew cabin as the initial cooling process of the cabin has just started, and the insufficient cooling capacity in the cabin due to the heat transfer from the engine compartment and the influence of solar radiation.

Figure 13 shows the comparison between the experimental and simulated values of the occupant compartment temperature under different scheme. The experimental conditions are the same as the constant speed and constant temperature conditions, and the boundary conditions are the same. The temperature of the passengers’ head (the temperature is the skin surface temperature) was compared in the cooling condition, and the simulation and the test were in good agreement, with the error within 1 °C. The simulated and test temperature curves at the passenger’s head position are in line with each other. As the vehicle air conditioner cools down, the passenger’s head drops and stabilizes, and the test value is slightly lower, with a temperature difference of about 1 °C.

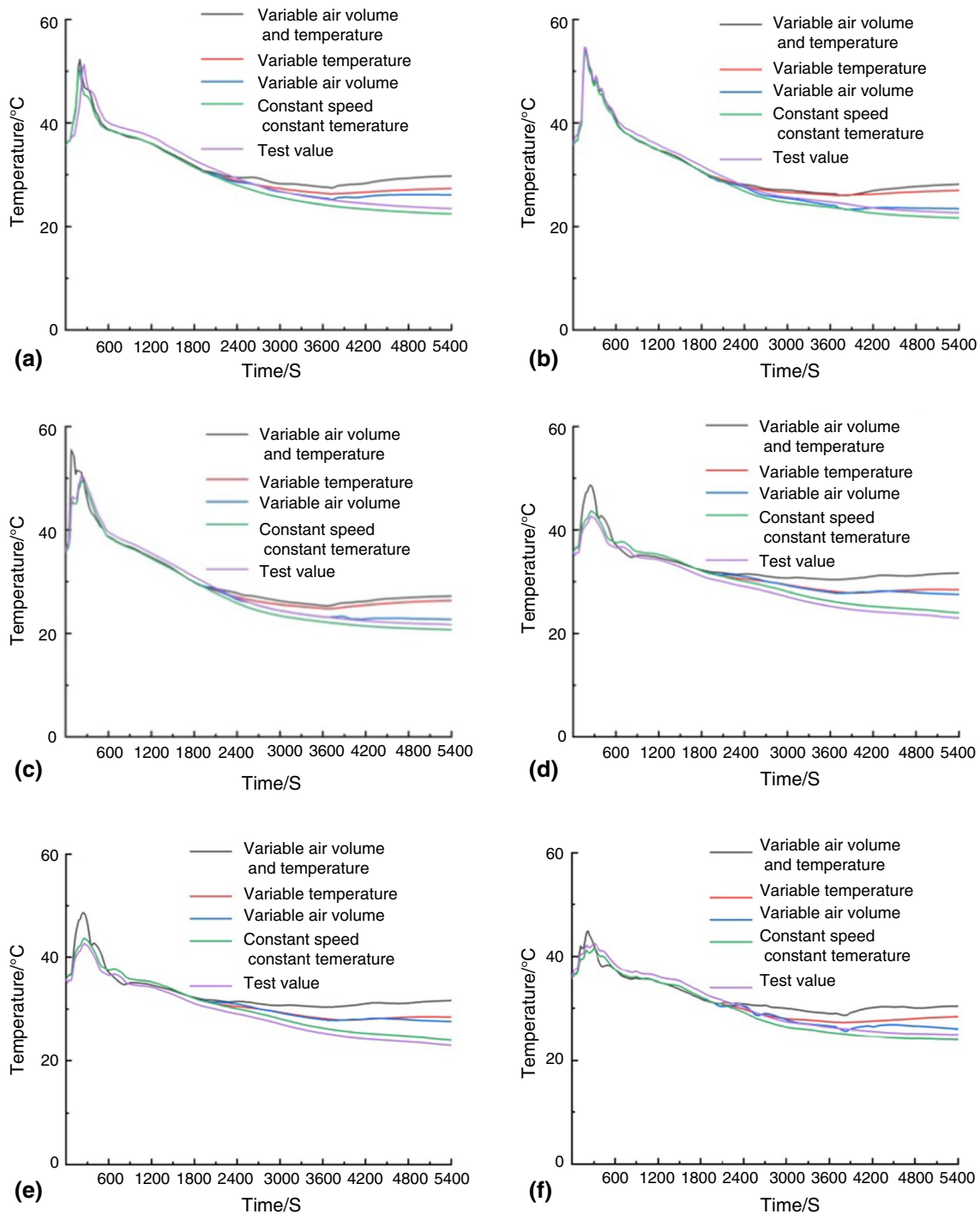


Fig. 13 Comparison of passenger head temperature under different scheme. **a** driver1, **b** passenger 1, **c** passenger 2, **d** passenger 3, **e** passenger 4 **f** passenger 5

Conclusion and future research work

Conclusion

Based on CFD simulation and theoretical analysis, the simulation study of variable air volume variable

temperature air supply strategy was conducted, and the velocity field, temperature field, and PMV-PPD index of the crew cabin with different air supply strategies were also compared and analyzed, and the following conclusions were obtained.

- (1) The temperature of the instrument panel of the crew cabin is too high and can be considered in reducing the heat transfer coefficient of the engine cabin bulkhead in front of the crew cabin, reducing the heat into the crew cabin, enhancing the overall thermal insulation performance of the instrument panel, while reducing the penetration rate of solar radiation of the windshield, which helps to reduce the heat load in the crew cabin, and has a certain degree of help to the cooling of the crew cabin. The temperature of the dashboard in scheme 1 was 24.9% lower than that of the dashboard in scheme 4.
- (2) The use of variable air volume delivery strategy can reduce the excess cooling capacity of the passenger compartment caused by the use of large mass flow rate and improve the thermal comfort level of the passenger compartment. Variable temperature air supply to the passenger compartment can reduce the phenomenon of low average radiation temperature in the passenger compartment caused by prolonged low-temperature air supply, and at the same time reduce the energy waste of the car caused by cooling. The passenger compartment for variable air volume air supply can avoid the cabin due to large air volume air supply caused by the waste of automotive energy, so that the cabin to obtain the appropriate wind speed. Scheme 1 combines the advantages of scheme 2 and scheme 3 to improve the thermal comfort level of the passenger compartment while saving a certain amount of energy in the vehicle. Scheme 1 increases the occupant compartment temperature by 43.2% compared to scheme 4, avoiding the reduction of thermal comfort in the passenger compartment due to the continuous low-temperature air supply.
- (3) Compared with scheme 2~scheme 4, the variable air volume and temperature air supply strategy of scheme 1 shows that the air velocity in the cabin will not be uncomfortable due to too high, the energy utilization efficiency is higher, and the mean radiation temperature in the occupant cabin will not be too low due to the air temperature, which indicates that the variable air volume and temperature air supply strategy makes the cooling capacity of the automobile air conditioner more fully utilized.

Future research work

The variable air volume and temperature strategy is transformed from single objective evaluation to multi-objective optimization. In this paper, only one evaluation index, PMV-PPD, is used, and multiple evaluation indexes are integrated in future work to provide the evaluation accuracy of thermal environment. Promote the development of the integration of air emission strategy and algorithm of vehicle air conditioner, and play the role of digital technology to provide

intelligent development of vehicle air conditioner. Improve the digitalization and intelligence of variable air volume and temperature air supply strategy. Integrate multiple evaluation criteria to improve the accuracy of evaluation. Accurately supply air to different areas of the passenger cabin. Digitalization, intelligence, and automation help to develop variable air volume and temperature air supply strategies.

Acknowledgements This project was supported by National Natural Science Foundation of China (51976012), by the scientific and technological project in Henan Province (222102240006), and also supported by Program for Innovative Research Team (in Science and Technology) in University of Henan Province (19IRTSTHN011).

References

1. Liu W, Ji W, Du X, et al. Investigation on numerical simulation of radiation heating thermal environment in car cabin. *J Phys: Conf Ser.* 2021;1838(1): 012055.
2. Jiong L, Liao S, Runming L. Analysis and research of thermal comfort of passenger cabin. *Automobile Parts.* 2019;1:1–5.
3. Liu W. Experimental and numerical study of the air distribution in an airliner cabin. *Dissertations & Theses—Gradworks.* 2014; 1565080.
4. Lee D, Lee H. Impact of focus- and diffuse-type air vents on cabin thermal comfort. *Int J Automot Technol.* 2020;21(5):1315–22.
5. Bhat A, Raghav G, Karn A. Implications of inlet vent design on air-distribution and thermal comfort inside a passenger car cabin. *SSRN Electr J.* 2019.
6. Zhou Z, Li J, Li M. Improvement and numerical simulation of air distribution in car indoor air conditioning environment. *Automob Appl Technol.* 2019;13:110–3.
7. Danca P, Vartires A, Dogeanu A. An overview of current methods for thermal comfort assessment in vehicle cabin. *Energy Procedia.* 2016;85:162–9.
8. Endoh H, Enami S, Izumi Y, et al. Experimental study on the effects of air flow from cross-flow fans on thermal comfort in railway vehicles: Volume VI: Transport ergonomics and human factors (TEHF), *Aerospace human factors and ergonomics.* 2019.
9. Zhang S, Lu Y, Lin Z. Coupled thermal comfort control of thermal condition profile of air distribution and thermal preferences. *Build Environ.* 2020;177: 106867.
10. Liu C, Li A, Yang C, et al. Simulating air distribution and occupants' thermal comfort of three ventilation schemes for subway platform. *Build Environ.* 2017;125:15–25.
11. Chang Z, Yi K, Liu W. A new ventilation mode of air conditioning in subway vehicles and its air distribution performance. *Energy Built Environ.* 2020;2(1):94–104.
12. Zhang Y, Liu J, Pei J, et al. Performance evaluation of different air distribution systems in an aircraft cabin mockup. *Aerosp Sci Technol.* 2017;70:359–66.
13. Khalil EE, ElDegwy AE. Passengers' thermal comfort in private car cabin in hot climate//2018 Joint Propulsion Conference. 2018; 4613.
14. Scurtu LI, Jurco AN. Airflow and thermal comfort of the bus passengers. *J Ind Des Eng Gr.* 2019;14(1):171–4.
15. Lee D, Lee H. Impact of focus-and diffuse-type air vents on cabin thermal comfort. *Int J Automot Technol.* 2020;21(5):1315–22.
16. Shin Y, Ham J, Cho H. Experimental study of thermal comfort based on driver physiological signals in cooling mode under summer conditions. *Appl Sci.* 2021;11(2):845.

17. Song C, Duan G, Wang D, et al. Study on the influence of air velocity on human thermal comfort under non-uniform thermal environment. *Build Environ*. 2021;196: 107808.
18. Ravindra K, Agarwal N, Mor S. Assessment of thermal comfort parameters in various car models and mitigation strategies for extreme heat-health risks in the tropical climate. *J Environ Manage*. 2020;267(3): 110655.
19. Yan-song HE, Jing L, Jie Y, et al. Experiment and simulation for occupant's surface temperature and thermal environment with human thermal regulation model. *China J Highw Transp*. 2021;34(1):199.
20. Hirn T, Kirmas A, Backes D, et al. The influence of radiation intensity and wavelength on thermal perception. *Build Environ*. 2021;196(5): 107763.
21. Liu W, Ji W, Du X, et al. Investigation on numerical simulation of radiation heating thermal environment in car cabin. *J Phys: Conf Ser*. 2021;1838(1): 012055.
22. Ye N, Zhuang L, Li N. A temperature control method for car room based on single user personalized comfort. *Chinese Intelligent automation conference*. Singapore; 2019. p. 373–81.
23. Tolis EI, Karanotas T, Svolakis G, et al. Air quality in cabin environment of different passenger cars: effect of car usage, fuel type and ventilation/infiltration conditions. *Environ Sci Pollut Res*. 2021;28(37):51232–41.
24. Schminder J, Gårdhagen R, Eek M, et al. Cockpit thermal comfort assessment using FMI models for co-simulations. *Center Mod-Based Cyber-Phys Prod Dev*. 2018;20(12):26–26.
25. Norrefeldt V, Mayer F, Herbig B, et al. Effect of increased cabin recirculation airflow fraction on relative humidity, CO₂ and TVOC. *Aerospace*. 2021;8(1):15.
26. Zhou X, Lai D, Chen Q. Thermal sensation model for driver in a passenger car with changing solar radiation. *Build Environ*. 2020;183: 107219.
27. Danca PA, Nastase I, Croitoru C, Bode F, Sandu M. Thermal comfort evaluation inside a car parked under sun and shadow using a thermal manikin. In: *IOP Conference Series: Earth and Environmental Science 2021 May 1 (Vol. 664, No. 1, p. 012064)*. IOP Publishing.
28. Qingqing W, Jianhua L. Comparative study on differences of human thermal characteristics in cabin between driving and idle state. *Heat Mass Transf*. 2020;56(7):2255–64.
29. Steiner A, Rauch A, Larrañaga J, et al. Energy efficient and comfortable cabin heating[M]//*Future interior concepts*. Cham: Springer; 2021. p. 89–100.
30. Horobet T, Danca P, Nastase I, et al. Preliminary research on virtual thermal comfort of automobile occupants//*E3S Web of conferences*. EDP Sci. 2018;32:01022.
31. Srinivasan Venkatesan L, Raina A. CFD Study of Different Aircraft Cabin Ventilation Systems on Thermal Comfort and Airborne Contaminant Transport: A Study on Passenger Thermal Comfort and Indoor Cabin Air Quality. 2020.
32. Cheung T, Schiavon S, Parkinson T, et al. Analysis of the accuracy on PMV–PPD model using the ASHRAE global thermal comfort database II. *Build Environ*. 2019;153:205–17.
33. Yang R, Zhang H, You S, et al. Study on the thermal comfort index of solar radiation conditions in winter. *Build Environ*. 2020;167: 106456.
34. Zhang S, He W, Chen D, et al. Thermal comfort analysis based on PMV/PPD in cabins of manned submersibles. *Build Environ*. 2019;148:668–76.
35. Danca P, Bode F, Nastase I, et al. CFD simulation of a cabin thermal environment with and without human body—thermal comfort evaluation//*E3S Web of Conferences*. EDP Sci. 2018;32:01018.
36. Yan-Kui WU, Zhu SY. An improved variable air volume air-conditioning system. *Build Energy Eff*. 2019;47(5):35–8.
37. Guo J, Meng X, Ma Q. Study on air supply control of marine variable-air-volume air-conditioning system. *Int J Comput Electr Eng*. 2019;11(2):108–17.
38. Wang B, Gao Y, Rui LI. Energy saving optimal control of variable water temperature and variable air volume in central air-conditioning system. *Mod Electr Tech*. 2019;42(5):141–4.
39. Moskvitina A, Shyshyna M, Korcheminskyi M. Feasibility study for the use of variable air volume systems for office buildings. *Vent Illum Heat Gas Supply*. 2021;36:62–79.
40. Kapalo P, Spodyniuk N. Effect of the variable air volume on energy consumption—case study. In: *IOP Conference Series: Materials Science and Engineering 2018 Aug 1 (Vol. 415, No. 1, p. 012027)*. IOP Publishing.
41. Ware YA, Khalighi B. Data-driven prediction of vehicle cabin thermal comfort: using machine learning and high-fidelity simulation results. *Int J Heat Mass Transf*. 2020;148: 119083.
42. Fiala D, Lomas KJ, Stohrer M. Computer prediction of human thermoregulatory and temperature responses to a wide range of environmental conditions. *Int J Biometeorol*. 2001;45(3):143–59.
43. Havenith G, Fiala D. Thermal indices and thermophysiological modeling for heat stress. *Compr Physiol*. 2015;6(1):255–302.
44. Chen J, Zheng X, Lan F, et al. An analysis on thermal comfort in passenger compartment based on human thermal regulation model. *Automot Eng*. 2019;41(6):723–30.
45. Rymuza K, Radzka E, Wierzycka G. Assessment of variation in thermal sensations determined based on effective temperature. *Journal of Ecological Engineering*. 2019;20(2):218–25.
46. Neacsu C, Tabacu I, Ivanescu M, et al. The evaluation of the overall thermal comfort inside a vehicle. *IOP Conf Ser: Mater Sci Eng*. 2017;252: 012031.
47. Wang L, Fan J. Modeling Bioheat Transport at Macroscale. *J Heat Transfer*. 2011;133(1): 011010.
48. Psikuta A, Allegrini J, Koelblen B, et al. Thermal manikins controlled by human thermoregulation models for energy efficiency and thermal comfort research—A review. *Renew Sustain Energy Rev*. 2017;78:1315–30.
49. Moon JH, Lee JW, Jeong CH, et al. Thermal comfort analysis in a passenger compartment considering the solar radiation effect. *Int J Therm Sci*. 2016;107:77–88.
50. Yang L, Li X, Tu J. Thermal comfort analysis of a high-speed train cabin considering the solar radiation effects. *Indoor Built Environ*. 2019;29(8):1101–17.
51. Chang TB, Sheu JJ, Huang JW, et al. Development of a CFD model for simulating vehicle cabin indoor air quality. *Transp Res Part D: Transp Environ*. 2018;62:433–40.
52. Aliahmadipour M, Abdolzadeh M, Lari K. Air flow simulation of HVAC system in compartment of a passenger coach. *Appl Therm Eng*. 2017;123:973–90.
53. Pang L, Li P, Bai L, et al. Optimization of air distribution mode coupled interior design for civil aircraft cabin. *Build Environ*. 2018;134:131–45.
54. UNE-EN ISO 7730–2006, Ergonomics of the thermal environment - Analytical determination and interpretation of thermal comfort using calculation of the PMV and PPD indices and local thermal comfort criteria (ISO 7730:2005).

Publisher's Note Springer Nature remains neutral with regard to jurisdictional claims in published maps and institutional affiliations.

Springer Nature or its licensor holds exclusive rights to this article under a publishing agreement with the author(s) or other rightsholder(s); author self-archiving of the accepted manuscript version of this article is solely governed by the terms of such publishing agreement and applicable law.